

Design and Performance of the Sorbent-Based Atmosphere Revitalization System for Orion

James A. Ritter, Steven P. Reynolds, and Armin D. Ebner

Department of Chemical Engineering, University of South Carolina
Columbia, SC, USA

James C. Knox

Marshall Space Flight Center, National Aeronautics and Space Administration
Huntsville, AL, USA

M. Douglas LeVan

Department of Chemical Engineering, Vanderbilt University
Nashville, TN, USA

ABSTRACT

Validation and simulations of a real-time dynamic cabin model were conducted on the sorbent-based atmosphere revitalization system for Orion. The dynamic cabin model, which updates the concentration of H₂O and CO₂ every second during the simulation, was able to predict the steady state model values for H₂O and CO₂ for long periods of steady metabolic production for a 4-person crew. It also showed similar trends for the exercise periods, where there were quick changes in production rates. Once validated, the cabin model was used to determine the effects of feed flow rate, cabin volume and column volume. A higher feed flow rate reduced the cabin concentrations only slightly over the base case, a larger cabin volume was able to reduce the cabin concentrations even further, and the lower column volume led to much higher cabin concentrations. Finally, the cabin model was used to determine the effect of the amount of silica gel in the column. As the amount increased, the cabin concentration of H₂O decreased, but the cabin concentration of CO₂ increased.

INTRODUCTION

Recent advances [1-7] in cyclic adsorption process modeling have revived the interests of NASA to assist them in the design and development of the next generation sorbent-based atmosphere revitalization (SBAR) system for water (H₂O) and carbon dioxide (CO₂) removal from spacecraft cabins. However, there are fundamental differences between Earth-bound and spacecraft cyclic adsorption processes. These subtle differences present some interesting challenges to the design of an SBAR system.

In space, vacuum is readily available. So, it is used to lower the partial pressures of the adsorbates in the bed to desorb them from a nearly saturated adsorbent. In contrast, on Earth dilutant gases are cheap. So, they are generally used as purge, which also effectively lowers the partial pressures of the adsorbates

in the bed to desorb them. Although a dilutant gas can certainly be used in spacecraft applications, the need for a continuous supply of it would be exorbitantly expensive. As a result, the development of cyclic adsorption processes for commercial and spacecraft needs has followed different paths, with extremely large pressure ratios generally replacing relatively high purge flows to foster bed regeneration. Finally, weight on the spacecraft is a critical issue. To reduce weight, a layered bed configuration is necessary.

The concept of a layered bed for a cyclic adsorption process is not new. A layered bed becomes of interest when components of very different adsorptivity need to be adsorbed from a feed stream [8]. The basic principle is to use a weak adsorbent at the inlet followed by stronger adsorbents to maximize the use of each adsorbent and to minimize the adsorber size [9].

One application for a pressure swing adsorption (PSA) process using a layered bed is air purification. Rege et al. [10] used a 1-bed, 4-step stripping PSA system to remove H₂O and CO₂ from an air feed. The adsorbents used in this study were activated alumina and zeolite 13X. It was shown that the H₂O concentration is optimum when the bed consisted of 75% activated alumina. The lowest CO₂ concentration occurred when the bed was 50% activated alumina. This showed that the activated alumina was needed for H₂O removal while the zeolite 13X was needed for CO₂ removal. Reynolds et al. [11] showed that air purification can be accomplished with a 2-bed 3-step PSA system utilizing deep vacuum without a light reflux step. The maximum CO₂ removal occurred with a layering of 50% silica gel, 17% zeolite 13X, and 33% zeolite 5A. With this layering, 100% of the H₂O and 88.0% of the CO₂ were removed for a 10 L column. However, both of these air purification studies allowed the system to come to a periodic state with a constant feed composition.

The new Crew Exploration Vehicle (CEV), Orion, will not operate at periodic conditions. Instead, the crew and the PSA system will experience real-time changes in the cabin concentrations for H₂O and CO₂.

astronauts, and the removal efficiency of the column. Figure 3 shows typical metabolic production rates during periods of rest, normal activity, exercise and normal activity for H₂O and CO₂ over a 24 hr period. The schedule is repeated for each day during a mission. As can be seen in the figure, there are two distinct regions of exercise. The first region is a period of aerobic

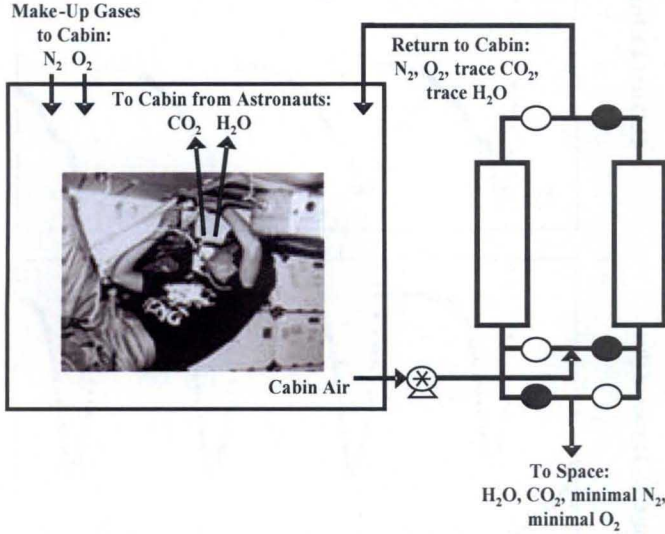


Figure 2. Schematic of the real-time dynamic cabin model used in the PSA-SBAR air purification study.

exercise, while the second region is a period of strength training. The PSA-SBAR system was in the feed step for 420 seconds out of a half cycle of 480 seconds, thus the fraction fed was 0.875. For 10 L columns in the PSA-SBAR system, the dynamic cabin model had average removal efficiencies of 100% for H₂O throughout the entire run and 83.0%, 82.9%, 79.6%, 77.6% and 79.4% for CO₂ during periods of rest, normal activity, aerobic exercise, strength exercise and normal activity, respectively. As shown in Figure 4, the cabin model was able to predict the steady state model values for H₂O and CO₂ for long periods of steady metabolic production. It also showed similar trends for the exercise periods, where there were quick changes in production rates.

Since the cabin model was validated against steady state predictions, a study was conducted to display the effect of the feed flow rate, and cabin and column volumes on the removal of H₂O and CO₂ generated from a 4-person crew with a given metabolic production schedule for a 4-day mission. The base case bed characteristics and operating parameters are shown in Table 1. The high pressure is set at atmospheric pressure, and the system is run with a high-to-low pressure ratio of 1,000. The crew size, initial feed composition, feed flow rate, feed and ambient temperatures, and overall heat transfer coefficient were provided by NASA. The cycle step times are similar to those used in a previous study [11], and the mass transfer coefficient for H₂O on silica gel was 0.002 s⁻¹.

The effects of flow rate (Q), cabin volume (V_{cab}), and column volume (V_{col}) on cabin H₂O and CO₂ concentrations (Figure 5) and PSA removal efficiencies (Figure 6) are illustrated with a 4-day mission for a 4-person crew with a H₂O and CO₂

metabolic production schedule shown in Figure 3. The bold and thin lines correspond to H₂O and CO₂, respectively. The dashed lines indicate the desired bounds (6 and 17.5 torr) for the H₂O cabin concentration. These bounds are set to eliminate any harm to the astronauts. If the H₂O

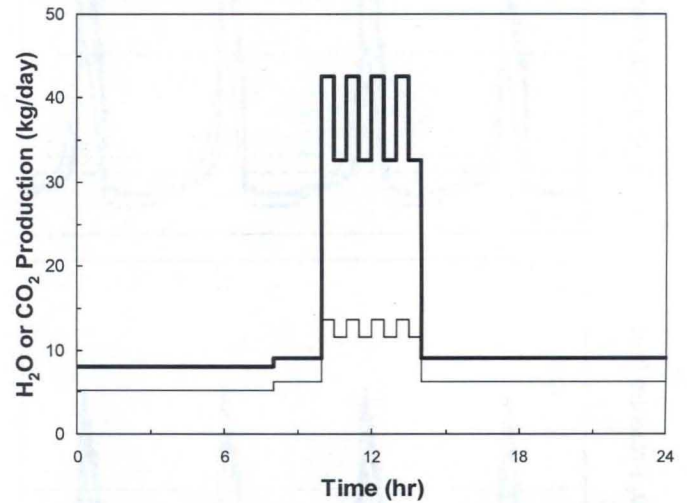


Figure 3. Typical metabolic production rates during periods of rest, normal activity, exercise and normal activity over a 24 hr period for a 4-person crew. Line styles: bold – H₂O; thin – CO₂.

Table 1. Bed characteristics and operating parameters utilized in the 4-person crew PSA-SBAR air purification study.

Bed Length (L)	0.244 m
Bed Radius (r _b)	0.081 m
Cabin Volume (V _{cab})	11 m ³
High Pressure (P _H)	101.325 kPa
Low Pressure (P _L)	0.101325 kPa
Crew Size	4
Initial Feed Mole Fraction: H ₂ O, CO ₂ ,	0.0125, 0.0021
O ₂ , N ₂	0.2083, 0.7771
Feed Flow Rate (Q _F)	700.00 SLPM
Feed Temperature (T _F)	291.48 K
Ambient Temperature (T _o)	291.48 K
Overall Heat Transfer Coefficient (h)	5.68x10 ⁻⁴ kJ/m ² s ⁻¹ K
Step Times (t _s): F,CnD, FP	420, 480, 60 s

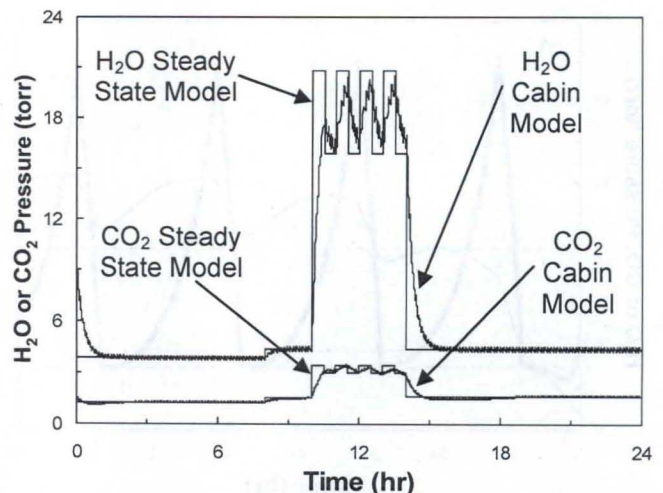


Figure 4. Validation run for the dynamic cabin model utilizing 10 L columns for the PSA-SBAR system.

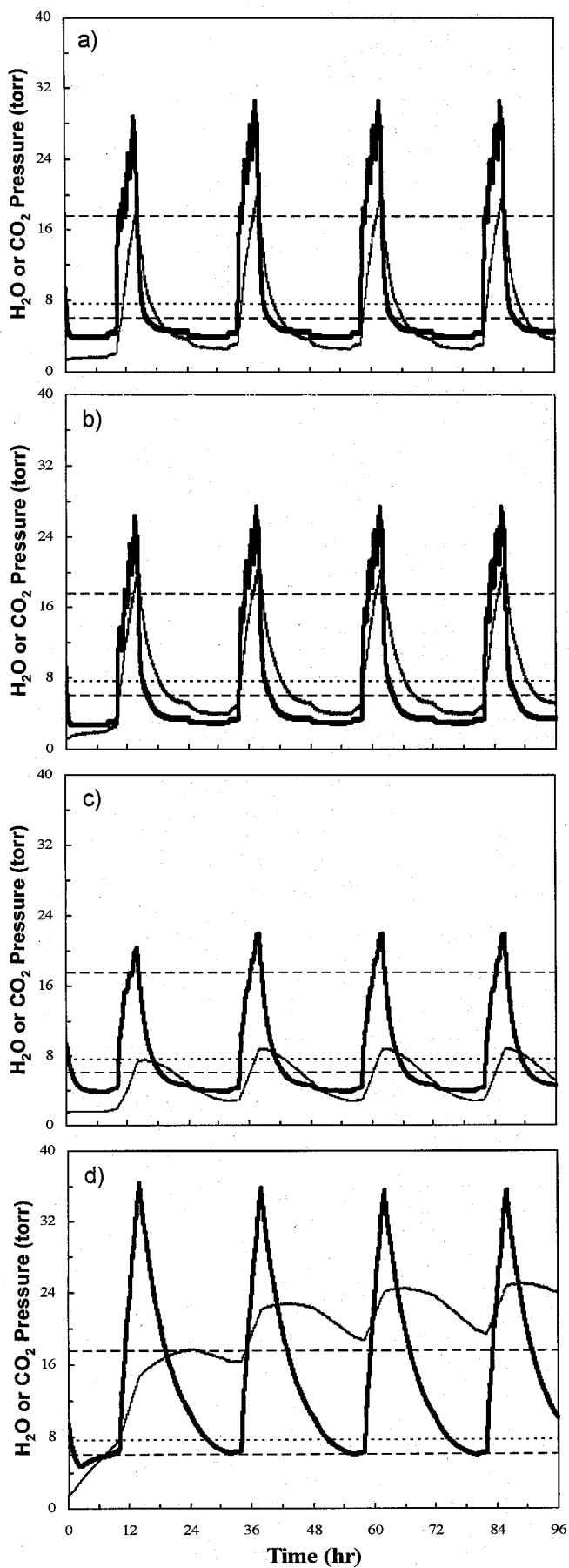


Figure 5. H₂O and CO₂ cabin concentrations from simulations of the dynamic cabin model for a) base case, b) effect of flow rate ($Q_F = 1000$ SLPM), c) effect of cabin volume ($V_{cab} = 44$ m³) and d) effect of column volume ($V_{col} = 2.5$ L). Line styles: bold – H₂O; thin – CO₂; dashed – H₂O bounds; dotted – CO₂ upper bound.

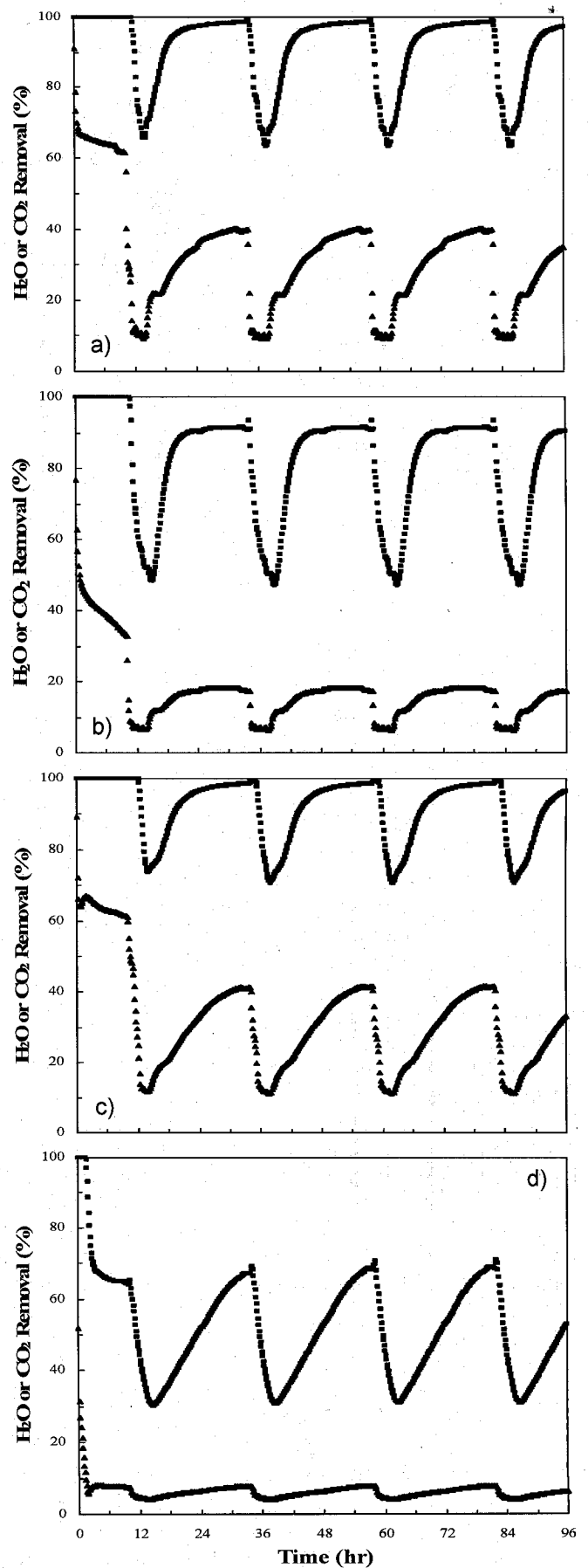


Figure 6. H₂O and CO₂ removal efficiencies from simulations of the dynamic cabin model for a) base case, b) effect of flow rate ($Q_F = 1000$ SLPM), c) effect of cabin volume ($V_{cab} = 44$ m³) and d) effect of column volume ($V_{col} = 2.5$ L). Symbols: squares – H₂O; triangles – CO₂.

concentration goes below the lower bound, the astronauts' skin will begin to crack. If the upper bound is exceeded, H₂O will begin to condense in the cabin. The dotted line indicates the safe upper bound (7.6 torr) for the CO₂ cabin concentration. If this bound is exceeded for an extended amount of time, it would be harmful to the astronauts.

Figure 5(a) shows the base case condition. It can be seen that during periods of rest and normal activity there was too little H₂O. At the same time the CO₂ was well below its bound. During these periods, the column was removing too much water and drying the cabin out. This can be avoided by slowing the feed flow rate down. However, during exercise periods the upper bounds for both H₂O and CO₂ were exceeded. As shown in Figure 6(a), the removal efficiency for both H₂O and CO₂ fell shortly after the exercise period began. The H₂O removal efficiency falling meant that the H₂O penetrated through the zeolite layers and returned to the cabin. Since the CO₂ was removed only by the zeolite layers, its removal efficiency fell as the H₂O was preferentially adsorbed by the zeolites. However, an interesting observation of Figure 5(a) was that the H₂O and CO₂ concentrations returned to the pre-exercise level within a few hours.

Figure 5(b) shows the H₂O and CO₂ concentrations for the effect of increasing Q to 1000 SLPM. Higher flow rates should lead to lower H₂O and CO₂ cabin concentrations. The concentrations of H₂O and CO₂ in the cabin were only slightly lower than those from the base case. A large decrease in the cabin concentrations was not observed due to the lower removal efficiencies of the PSA unit as shown in Figure 6(b).

Figure 5(c) shows the effect of increasing the V_{cab} to 44 m³. The H₂O and CO₂ cabin concentrations were reduced, even though the removal efficiencies were similar to the base case. The concentrations, however, still exceeded the upper bounds. But, this did not happen until much later in the exercise period. The larger cabin led to a slower response, which dampened the large variations observed in Figure 5(a).

Table 2. Bed characteristics and operating parameters utilized in the 6-person crew PSA-SBAR air purification study.

Bed Length(L)	0.244 m
Bed Radius (r _b)	0.081 m
High Pressure (P _H)	101.325 kPa
Low Pressure (P _L)	0.101325 kPa
Crew Size	6
Initial Feed Mole Fraction: H ₂ O, CO ₂ ,	0.0125, 0.0033,
O ₂ , N ₂	0.2083, 0.7759
Feed Flow Rate (Q _F)	849.51 SLPM
Feed Temperature (T _F)	294.26 K
Ambient Temperature (T _a)	294.26 K
Overall Heat Transfer Coefficient (h)	5.68x10 ⁻⁴ kJ/m ² s K
Step Times (t _s): F,CnD, FP	420, 480, 60 s

Figure 5(d) shows the effect of decreasing V_{col} to 2.5 L. The cabin concentrations were dramatically

higher than that observed for the base case. In fact, the CO₂ concentration never came to a periodic state. The smaller column led to lower removal efficiencies resulting in higher H₂O and CO₂ cabin concentrations.

The second study performed on this system consisted of a 6-person crew undertaking ground operations and a 3-day mission to dock the Orion with the ISS. Ground operations consisted of a 6 hour period of time prior to launch. Throughout the ground operations the PSA-SBAR system was run at atmospheric conditions with one system undergoing the F step and the other system undergoing a purge step that consisted of N₂ flowing in a countercurrent direction to remove H₂O and CO₂ from the adsorbent layers. After ground operations, there was essentially no H₂O or CO₂ on the adsorbents due to the N₂ purge.

Table 2 shows the conditions used for the 5 simulations run in this study. The initial feed mole fraction is the concentration of the components in the cabin at the start of ground operations. The mass transfer coefficient for H₂O on silica gel was 0.029 s⁻¹. This number was used as a conservative estimate of results from recent experiments not shown here. The metabolic production schedule is shown for one day in Figure 7. Again, this schedule is repeated every day during the mission. Since there are 6 crew members and a short mission, no exercise is required.

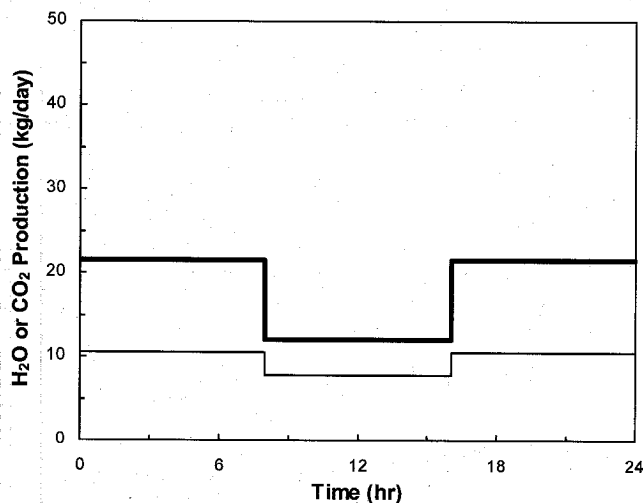


Figure 7. Typical metabolic production rates during periods of normal activity, rest and normal activity over a 24 hr period for a 6-person crew. Line styles: bold – H₂O; thin – CO₂.

Figure 8 shows the H₂O and CO₂ cabin concentrations for ground operations followed by a 3-day mission to the ISS, while Figure 9 shows the removal efficiencies of H₂O and CO₂ and the loss of O₂ and N₂ to space for only the 3-day mission. The first 6 hours of Figure 8 correspond to the ground operations. It can be seen that the H₂O and CO₂ came to a periodic state in the cabin and that the levels in the cabin were well within the bounds for each component. The H₂O concentration in the cabin fell below the lower bound during the rest period for each of the 3 days. This was due to the high flow rate being held constant throughout the entire run. To keep the H₂O level above the lower bound, the flow rate can be reduced during periods of

rest. However, the CO₂ concentration went above its safe upper limit during the second day of normal activity. This was due to H₂O penetrating into the zeolite layers. Water preferentially adsorbed to the zeolite, thus CO₂ was not able to adsorb and be removed from the feed stream. This can be seen in Figure 9 as the CO₂ removal efficiency continuously declined until about 40 hours into the 3-day mission. One last observation from Figure 8 is that the H₂O concentration began to increase in the cabin after approximately 58 hours of operation (52 hours into the mission). This was due to H₂O breaking through the column and returning to the cabin in the PSA effluent stream. This observation corresponded with the drop in the removal efficiency of H₂O shown in Figure 9.

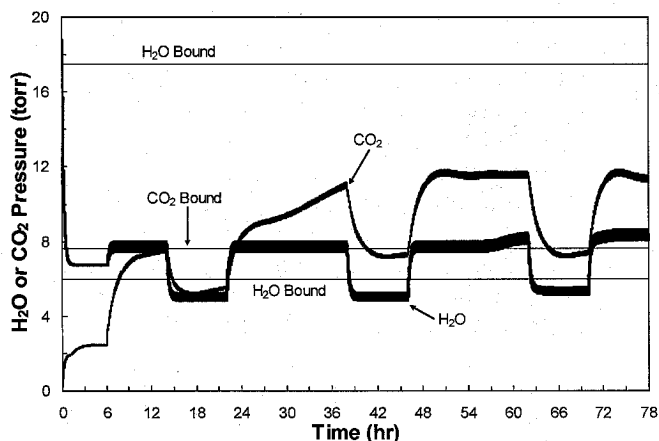


Figure 8. H₂O and CO₂ cabin concentrations for ground operations and a 3-day mission to the ISS for a system containing 50% silica gel.

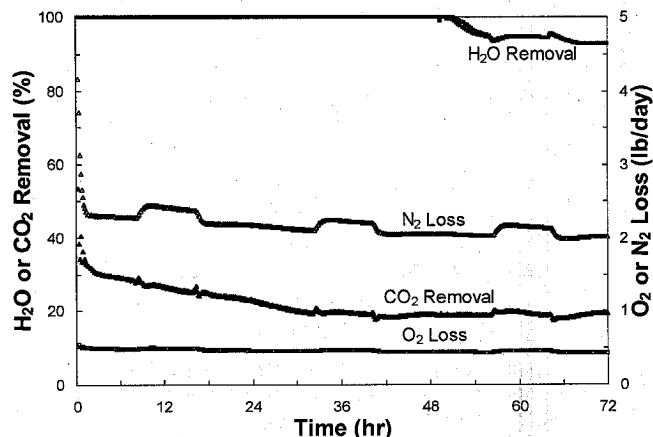


Figure 9. H₂O and CO₂ removal efficiencies and O₂ and N₂ losses for a 3-day mission to the ISS for a system containing 50% silica gel. Symbols: squares – H₂O removal efficiency; triangles – CO₂ removal efficiency; empty squares – O₂ loss; empty triangles – N₂ loss.

The effect of the amount of silica gel in the PSA-SBAR column on the H₂O and CO₂ cabin concentrations were difficult to see in a graph similar to Figure 8. There were only slight differences between the cabin concentrations achieved with 35% and 55% silica gel. However, the differences can be seen with graphs similar to Figure 9. Thus, Figures 10 and 11 show the effect of the amount of silica gel in the PSA-SBAR column on the removal efficiencies of H₂O and CO₂.

As the silica gel percentage increased in the

column, the H₂O removal efficiency remained higher throughout the run as shown in Figure 10. Since the silica gel was used as the bulk H₂O remover, more silica gel in the column led to more H₂O being removed. This, in turn, meant that less H₂O needed to be adsorbed by the zeolite layers. Thus, breakthrough of the H₂O occurred later in the run for the columns containing more silica gel. Therefore, the H₂O concentration in the cabin was slightly lower for the columns containing more silica gel.

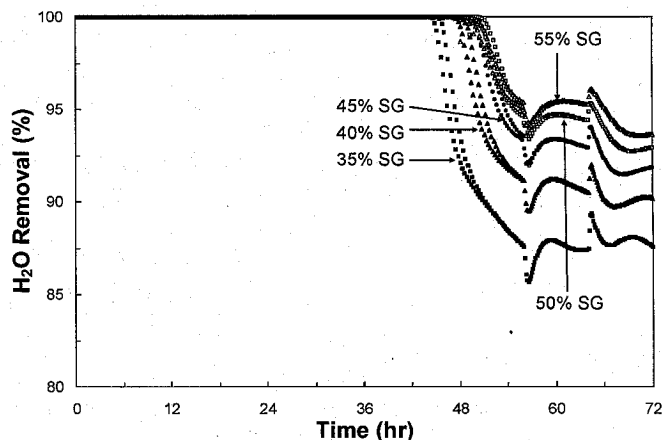


Figure 10. H₂O removal efficiency for a 3-day mission for the CEV to dock with the ISS. Symbols: squares – 35% silica gel; triangles – 40% silica gel; circles – 45% silica gel; empty squares – 50% silica gel; empty triangles – 55% silica gel.

Figure 11 shows the CO₂ removal efficiency throughout the 3-day mission as a function of the silica gel percentage. The silica gel had an opposite effect on the CO₂ as it did on the H₂O. For CO₂, the removal efficiency decreased as the silica gel percentage increased. This was caused by the fact that as the silica gel percentage increased the percentage of zeolite 13X decreased. Since the CO₂ was removed only by the zeolite layers, the capacity to remove the CO₂ from the feed stream was decreased as the zeolite 13X amount was decreased. Therefore, the cabin concentration of CO₂ increased as the silica gel percentage increased.

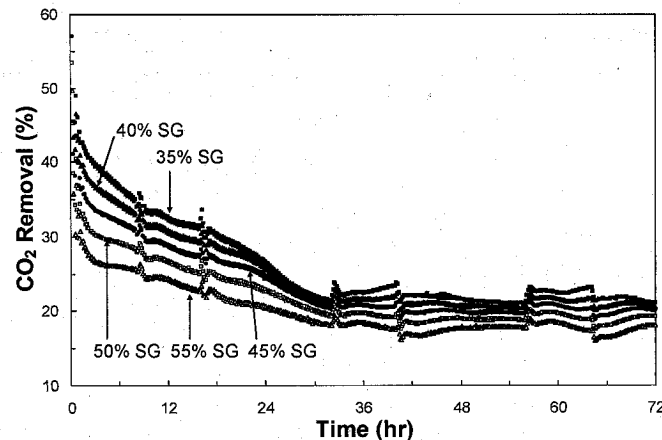


Figure 11. CO₂ removal efficiency for a 3-day mission for the CEV to dock with the ISS. Symbols: squares – 35% silica gel; triangles – 40% silica gel; circles – 45% silica gel; empty squares – 50% silica gel; empty triangles – 55% silica gel.

CONCLUSIONS

A rigorous cabin model was developed to aid in the design and development for the SBAR system on the new CEV, Orion. This cabin model was able to update the cabin concentrations of H₂O and CO₂ every second throughout the run. It was validated against a steady state model that was based only on the total flow, the fraction of time that one of the columns was undergoing the F step, the metabolic rate of the astronauts, and the removal efficiency of the column. The dynamic cabin model was able to predict the steady state model values for H₂O and CO₂ for long periods of steady metabolic production. It also shows similar trends for the exercise periods, where there are quick changes in production rates.

Once validated, the dynamic cabin model was used to illustrate the effect of flow rate, cabin volume and column volume on the cabin concentrations of H₂O and CO₂ for a 4-person crew over a 4-day period. Increasing the flow rate led to slightly lower cabin concentrations of H₂O and CO₂ since more of these components are able to interact with the adsorbent. The expected decrease in the cabin concentrations was not observed as the removal efficiency for both H₂O and CO₂ was much lower than the base case.

An increase in the cabin volume caused a reduction in the H₂O and CO₂ cabin concentrations, even though the removal efficiencies were similar to the base case. The larger cabin led to a slower response, which dampened the large variations observed in the base case. A smaller column adsorbed less H₂O and CO₂ than the base case which resulted in dramatically larger cabin concentration than the base case. In fact, the CO₂ concentration never came to a periodic state. The smaller column led to lower removal efficiencies resulting in higher H₂O and CO₂ cabin concentrations.

Finally, the cabin model was used to observe the effect of the silica gel percentage in the column on the concentrations of H₂O and CO₂. As the silica gel percentage increased in the column, the H₂O removal efficiency remained higher throughout the run. Thus, breakthrough of the H₂O occurred later in the run for the columns containing more silica gel. Therefore, the H₂O concentration in the cabin was slightly lower for the columns containing more silica gel. The silica gel, though, had an opposite effect on the CO₂ as it did on the H₂O. For CO₂, the removal efficiency decreased as the silica gel percentage increased. This was caused by the fact that as the silica gel percentage increased the percentage of zeolite 13X was decreased. Thus, the capacity to remove the CO₂ from the feed stream was decreased as the zeolite 13X amount was decreased. Therefore, the cabin concentration of CO₂ increased as the silica gel percentage increased.

ACKNOWLEDGEMENTS

Financial support for this work provided by the NASA MSFC was greatly appreciated.

REFERENCES

1. Ebner, A.D., and J.A. Ritter, "Equilibrium Theory Analysis of a Rectifying Pressure Swing Adsorption Process for Producing Pure Heavy Component," *AIChE J.*, **48**, 1679-1691 (2002).
2. McIntyre, J.A., C.E. Holland, and J.A. Ritter, "High Enrichment and Recovery of Dilute Hydrocarbons by Dual Reflux Pressure Swing Adsorption," *Ind. Eng. Chem. Res.*, **41**, 3499-3504 (2002).
3. Daniel, K.D., and J.A. Ritter, "Equilibrium Theory Analysis of a Pressure Swing Adsorption Cycle Utilizing an Unfavorable Langmuir Isotherm. 1. Periodic Behavior," *Ind. Eng. Chem. Res.*, **41**, 3676-3687 (2002).
4. Liu, Y., J.A. Ritter, and B.K. Kaul, "Pressure Swing Adsorption Cycles for Improved Solvent Vapor Enrichment," *AIChE J.*, **46**, 540-551 (2000).
5. Liu, Y., C.E. Holland, and J.A. Ritter, "Solvent Vapor Recovery by Pressure Swing Adsorption. III. Comparison of Simulation with Experiment for the Butane-Activated Carbon System," *Sep. Sci. Tech.*, **34**, 1545-1576 (1999).
6. Ritter, J.A., Y. Liu, and D. Subramanian, "New Vacuum Swing Adsorption Cycles for Air Purification with the Feasibility of Complete Clean-Up," *Ind. Eng. Chem. Res.*, **37**, 1970-1976 (1998).
7. Liu, Y., and J.A. Ritter, "Evaluation of Model Approximations in Simulating Pressure Swing Adsorption-Solvent Vapor Recovery," *Ind. Eng. Chem. Res.*, **36**, 1767-1778 (1997).
8. Chlendi, M., and D. Tondeur, "Dynamic Behaviour of Layered Columns in Pressure Swing Adsorption," *Gas. Sep. Purif.*, **9**, 231-242 (1995).
9. Park, J.-H., J.-N. Kim, S.-H. Cho, J.-D. Kim, and R.T. Yang, "Adsorber dynamics and optimal design of layered beds for multicomponent gas adsorption," *Chem. Engng. Sci.*, **53**, 3951-3963 (1998).
10. Rege, S.U., R.T. Yang, K. Qian, and M.A. Buzanowski, "Air-Prepurification by Pressure Swing Adsorption Using Single/Layered Beds. *Chem. Eng. Sci.*, **56**, 2745-2759 (2001).
11. Reynolds, S. P., A. D. Ebner, and J. A. Ritter, "Novel Layered Bed PSA Cycle for CO₂ and H₂O Removal from Air Utilizing Deep Vacuum and No Light Reflux," *Sep. Sci. Tech.*, submitted (2007).

CONTACT

E-mail: ritter@enr.sc.edu